

Effects of Synthesized Superparamagnetic Iron Oxide Nanoparticles and Extremely Low Frequency

Mohammad Satari^{1*}, Nazanin Haghghat¹, Fatemeh Javani Jouni¹, Parviz Abodolmaleki¹

¹ Department of Biophysics, Faculty of Biological Science, Tarbiat Modares University, Tehran, Iran

* Corresponding author: Parviz Abodolmaleki, Department of Biophysics, Faculty of Biological Science, Tarbiat Modares University, Tehran, Iran. E-mail: parviz@modares.ac.ir

DOI: 10.30699/acadpub.mci.2.1.2

Submitted: 17 August 2017

Revised: 10 October 2017

Accepted: 25 December 2017

ePublished: 01 January 2018

Keywords:

Superparamagnetic Iron Oxide

Extremely Low-Frequency

Magnetic Fields (ELMFs)

X-ray Diffraction

Abstract

Introduction: Iron oxide nanoparticles, owing to their very small size and superparamagnetic properties, have been considered a potential candidate for several medical applications such as magnetic cell separation, magnetic resonance imaging (MRI), magnetic targeted drug delivery magnetic hyperthermia. The present study aimed to synthesize and evaluate the characteristics of superparamagnetic iron oxide nanoparticles (SPIONs) and determine the mechanism by which they induce cell death in the presence of an extremely low-frequency magnetic field (ELMF).

Methods: First, SPIONs were synthesized using the chemical co-precipitation method and then characterized by X-ray diffraction (XRD), transmission electron microscopy (TEM), dynamic light scattering (DLS), and zeta potential. A vibrating-sample magnetometer (VSM) was used to measure the magnetic properties of the nanoparticles. Human MCF-7 breast cancer cells were treated with different concentrations of SPION in the absence and presence of a 50-Hz ELMF for 24 and 48 h. Cytotoxicity and cell viability percentage in the treated cells were measured by the MTT (3-(4,5-dimethylthiazol-2-yl)-2,5-diphenyltetrazolium bromide) assay.

Results: DLS and TEM analyses indicated that the SPIONs have an average size of less than 30 nm and they are superparamagnetic. VSM analyses also confirmed the superparamagnetic nature of the nanoparticles. The MTT assay indicated that high concentrations of SPIONs induced death in MCF-7 cells. In the groups treated with ELMF+SPIONs, cell death increased sharply compared with that in the groups treated with each treatment alone ($P \leq 0.05$).

Conclusions: It seems that a 50-Hz ELMF in the presence of SPIONs led to cell death due to local heating

© 2018. Multidisciplinary Cancer Investigation

INTRODUCTION

The reduction in the size of iron oxide nanoparticles causes an increase in their surface-to-volume ratio. The large surface area of magnetic nanoparticles dramatically changes their magnetic properties. Iron oxide nanoparticles smaller than 30 nm can be considered to have a single magnetic domain. They exhibit superparamagnetic properties and are hence called superparamagnetic iron oxide nanoparticles (SPIONs). SPIONs exhibit extraordinary magnetic properties in the presence of an external magnetic field; they quickly reach magnetic saturation and do not retain any magnetism after the external magnetic field has been removed. This property prevents them

from accumulating in the capillaries and causing blockage [1]. The attractive properties of SPIONs such as super-paramagnetic, high-field irreversibility, and high saturation field have made them ideal candidates for biomedical applications such as contrast agents for magnetic resonance imaging (MRI), targeted drug delivery in tumor therapy [2, 3] and hyperthermia [4], controlled release of drugs [5], and targeting gene delivery or magnetofection [6, 7]. Cancer is a group of diseases characterized by uncontrolled cell growth and the possibility of metastasis [8]. Breast cancer has the highest mortality after lung cancer worldwide and is the most common-

cause of death in American females [8]. The patients with metastatic breast cancer are classified based on receptor status of progesterone and estrogen receptors (PR/ER) and human epidermal growth factor receptor 2 (HER2), which is also known as the breast cancer pre-diagnosis indicator. A clinical assessment of these indicators may take several months to up to several years [9]. Metastatic tumors with negative ER/PR and negative HER2 are considered triple negative. About 13% of all breast cancers are triple negative which are often reversible after primary treatment and susceptible to further progress. Therefore, hormonal therapy involving tamoxifen and aromatase inhibitors is not effective in such patients [10]. Some studies have shown that only 40% of the metastatic tumors with PR/ER receptors respond to medicines such as tamoxifen. Among them, most of the patients develop drug resistance during the treatment process, which makes successful treatment difficult [11, 12]. Therefore, developing other treatments that do not depend on cell receptors such as those using magnetic and electromagnetic fields (EMFs) can be useful to treat this type of cancer.

When creating a static magnetic field, the electric current direction does not change with time, whereas creating an EMF changes the electric current direction in a wire tube with time. Extremely low-frequency magnetic field (ELMF) is the type of EMF with a frequency range from 50 to 60 Hz. ELMF is known to induce a weak electric current in the human body. ELMF does not have sufficient energy to break DNA molecules and is therefore known as “nonionizing radiation.” However, ELMF affects biomolecules such as the DNA by increasing the number of reactive oxygen species [13], which affect signal transduction pathways, cell cycle, and gene expression, and eventually cause apoptosis. Moreover, ELMF causes distortion of chemical bonds imposes a force on ions and small ligands, causes conformational changes in membrane proteins, and causes the export of ions especially calcium ions from the cells [14, 15].

EMF can be used as a co-treatment in cancer therapy. A combination of EMF and gamma radiation was found to significantly reduce tumor growth and vascularization in human breast cancer cells [16]. EMF is also used in magnetic hyperthermia in combination with magnetic nanoparticles. In this method, SPIONs are injected in the form of a ferrofluid into the target cells; then, the EMF in the megahertz range is applied to the cells or the target tissue [17]. SPIONs absorb the force of the EMF and convert it into heat by increasing internal vibrations as a result of hysteresis and relaxation losses [18]. However,

the risk of local overheating and subsequent damage to normal tissues is the main challenge concerning magnetic hyperthermia [19]. An alternative method that may help solve this challenge is the application of low-frequency EMF (50 Hz) and using SPIONs for longer intervals simultaneously. In other words, we hypothesize that decreasing EMF frequencies (up to 50 Hz) and increasing EMF exposure in the presence of SPIONs can induce death in cancer cells.

The present study investigated the ability of a 50-Hz EMF and SPIONs to induce death in MCF-7 breast cancer cells. For this, superparamagnetic nanoparticles were synthesized and characterized, and their structural and functional characteristics were examined. Thereafter, the mortality of MCF-7 breast cancer cells treated with various concentrations of SPIONs in the presence and absence of a 50-Hz EMF at different time exposure was studied.

METHODS

Synthesis of Fe₃O₄ Nanoparticles

Ferrous chloride (FeCl₂·4H₂O) and ferric chloride (FeCl₃·6H₂O) of 99% purity were purchased from Merck Company (Germany). Magnetic nanoparticles were synthesized by the co-precipitation method. The reaction was conducted in the presence of N₂ and absence of O₂ to prevent oxidation. Initially, 4 mmol FeCl₂·6H₂O and 2 mmol FeCl₂·4H₂O were dissolved in 40 mL deionized water. While the solution was stirred using a mechanical stirrer vigorously, 25% ammonia solution was added dropwise until the solution reached the pH value of 11. Stirring was continued for 1 h at 70°C in the presence of N₂. Then, the solution was cooled at room temperature, sediments were separated using a permanent magnet and washed several times with deionized water and ethanol until reached a neutral pH. Finally, the precipitate of the magnetic nanoparticles was washed with acetone and dried at 60 to 70°C in an oven. The nanoparticle-forming reaction is shown in Equation 1 [20].



Characteristics and Morphology of the Nanoparticles

After synthesizing the nanoparticles, the hydrodynamic distribution of the particles was assessed by dynamic light scattering (DLS). First, the particles were suspended in deionized water and sonicated by using an ultrasonic bath for 30 min. Then, the nanoparticles were prepared at final concentration of 10 µg/mL

and nanoparticle size distribution was analyzed with Zetasizer Nano ZS instrument (Malvern Instruments Ltd, Malvern, Worcestershire, UK). Results obtained from DLS showed that the average size of particles were suitable and the hydrodynamic size was about 32 nm (Figure 1a). Transmission electron microscopy (TEM)—a powerful instrument to examine the structure, composition, and properties of nanoparticles—was used to determine the shape and size of the nanoparticles. TEM images of the nanoparticles showed that the particles were spherical and about 10 nm in size (Figure 2). The results also showed that the synthesized particles were super-paramagnetic in nature.

The crystal structure of nanoparticles was examined by X-ray diffraction (XRD). As shown in Figure 3, the XRD patterns indicated seven characteristic peaks at 2θ equal to 21.5° , 35.4° , 41.7° , 50.9° , 63.7° , 68.0° , and 75.1° , which corresponded to the Miller indices values $\{hkl\}$ of $\{111\}$, $\{220\}$, $\{311\}$, $\{400\}$, $\{422\}$, $\{511\}$, and $\{440\}$ of Fe_3O_4 nanoparticles, respectively. These results revealed that the crystal structures of the synthesized nanoparticles fully correlated with those of Fe_3O_4 nanoparticles.

Magnetic Behavior of Nanoparticles

The magnetic behavior of the synthesized SPIONs was examined by using a vibrating sample magnetometer (VSM) and its results in 298 K and 10^{10} Oe as shown in Figure 4. The magnetic hysteresis loop was entirely reversible, which proved its super-paramagnetic characteristic. In other words, by increasing the intensity of the external magnetic field, the magnetization in these particles increased, and after the removal of the external magnetic field, a

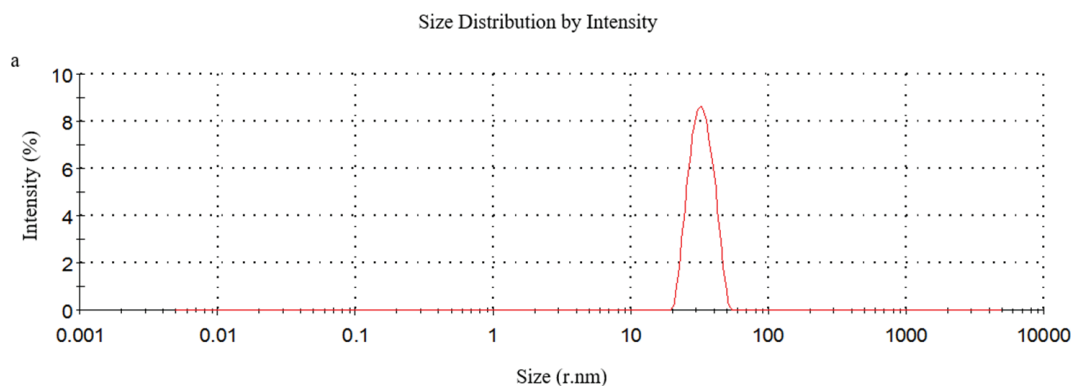
decrease in magnetization occurred precisely via the same pathway and completely lost its magnetic property. Therefore, it is expected to maintain the colloidal stability of the particles and prevent their accumulation and bonding in the absence of external magnetic field [21, 22].

Cell Culture

The human breast cancer cell line MCF-7 was purchased from Iran Pasture Institute and cultured at $37^\circ C$, 5% CO_2 in the Dulbecco's Modified Eagle's Medium (DMEM) medium supplemented with 10% fetal bovine serum (FBS), 100 U/mL of penicillin, and 100 mg/mL of streptomycin. The cells were grown until they reached 70% to 80% confluency. The cells were then re-passaged every three or four days at a ratio of 1:2 and 1:3 using 0.25% trypsin (Invitrogen LT, Merelbeke, Belgium). Thereafter, the cells were frozen in the DMEM environment with 93% FBS and 7% dimethyl sulfoxide (DMSO MERCK, Darmstadt, Germany).

Low-Frequency Magnetic Field Device

Exposure to ELMF was performed using a locally designed ELMF generator. The magnetic field generator consisted of two coils connected to the urban electrical power (220 V, 50 Hz). The coils were built using a 3-mm diameter wire that was resistant to heat to up to $200^\circ C$. Wire length in each coil was about 1 km and each coil weighed approximately 40 kg. The coils had a total resistance of $3\ \Omega$ and an inductance of 2 H. The intensity of the magnetic field created around the coil varied, and the highest magnetic field intensity reached up to 500 mT when concentrated in a small area.



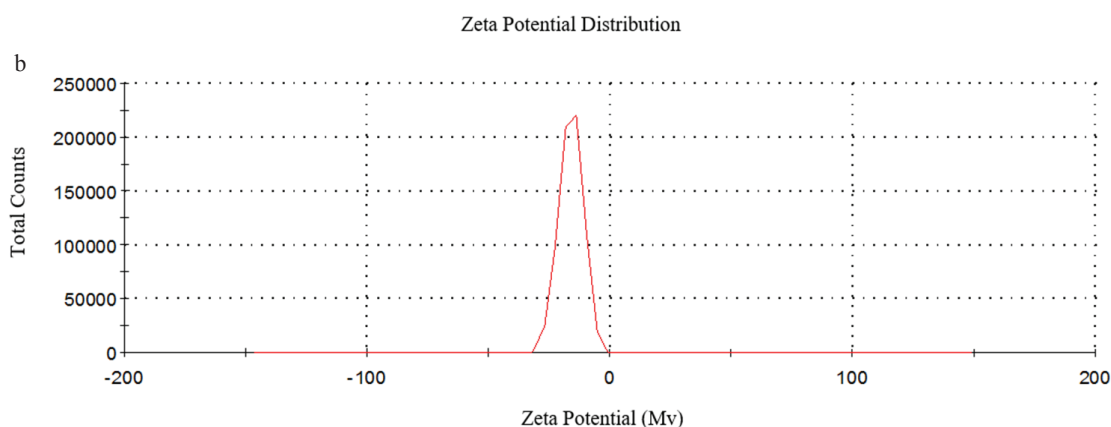


Figure 1: The Results Obtained from DLS. The particle size distribution chart showing that a) the average particle size was about 32 nm, and b) the surface charge of the nanoparticles was about -19 mV.

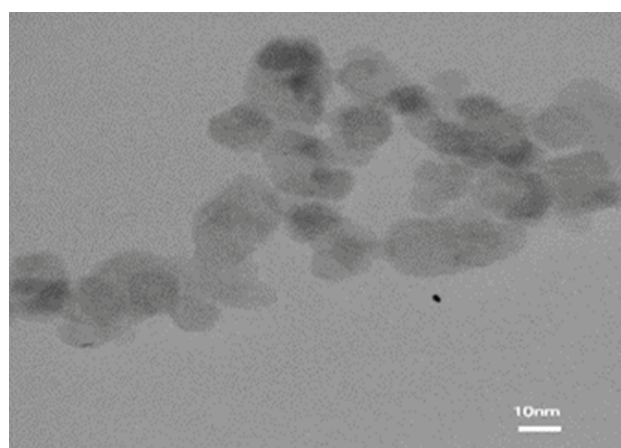


Figure 2: A TEM Image Showing That the Size of SPION Was About 10 nm.

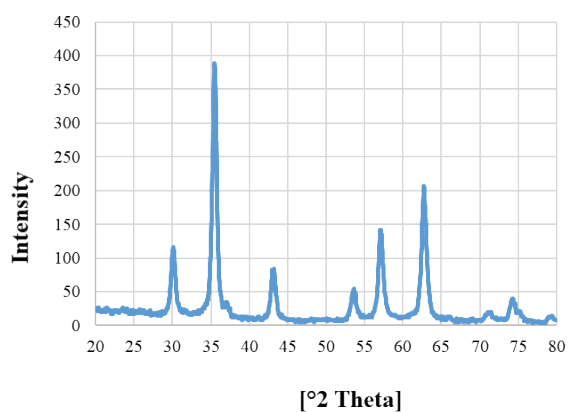


Figure 3: The Diffraction Pattern of the Obtained X-ray Showing the SPION Magnetic Structure.

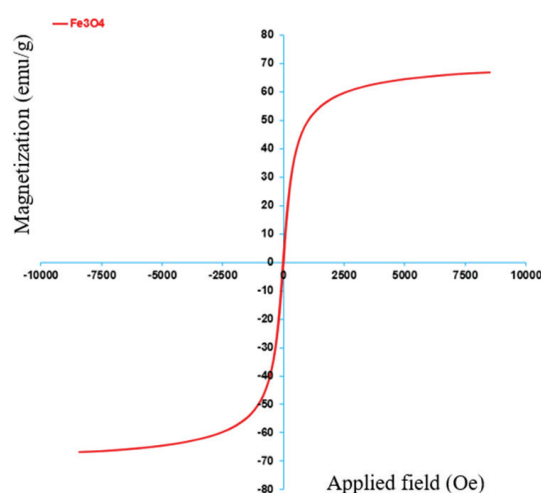


Figure 4: The Obtained VSM Curve Showing the Paramagnetic Behavior of SPION Particles.

To use more space and intensify the field, the magnetic field was transferred to a U-shaped blade that was 1 m high and had cross sections of 10 cm made using iron sheets that were separated by thin layers of mica. The intensity of the magnetic field created on this blade varied from 0.5 to 30 mT depending on the voltage and current intensity of the wire. By connecting the field plug to AC, an alternative magnetic field was created with 50 Hz frequency and 20 mT, which, unlike the static magnetic field, did not have direct magnetism and was oscillated with the magnet close to it. A hand-made incubator with

a 40-cm height was equipped with devices that regulated the temperature, humidity, and CO₂ pressure. This incubator was connected to a CO₂ capsule and the culture plates in standard conditions were placed (37°C and 5% CO₂ pressure and appropriate moisture). The body of the incubator was made using plastic sheets without pores for ease of sterilization (Figure 5). To regulate the device and measure the intensity of the magnetic field created by it, the Gottingen PHYWE tesla meter model 13610-93 (Germany) with 10% accuracy was used. Any changes in the input current of the device were measured using an oscilloscope (40 MHz, model 18040-leader; Japan). To control the heat, the side walls of the incubator were fitted with a wired heater that was attached to the thermostat and the temperature was kept constant at 37 °C. To regulate the pressure of CO₂, an infrared sensor was also used inside the incubator that showed the gas pressure on a special monitor. The enclosure was connected by a gas hose to a CO₂, which controlled the gas pressure by regulator valves.



Figure 5: The Magnetic Field Device. The coils, u-shaped blade (Yellow), and an incubator were placed within the exposure chamber. The incubator was equipped with sensors of temperature, humidity, and CO₂ pressure.

MTT Assay

MTT (3-(4,5-dimethylthiazol-2-yl)-2,5-diphenyltetrazolium bromide) assay was performed to measure cell viability. When the cells reached 70% to 80% confluency, they were harvested via trypsinization and seeded in the complete medium in a 96-well tissue culture plate at a density of 10⁴ cells in 100 µL medium per well and incubated for 24 h (37°C, 5% CO₂). The cells were then divided into four groups: 1- Control cells without any treatment; 2- Cells exposed to a 50-Hz ELMF with 20 mT intensity for 24 and 48 h; 3- Cells treated only with different concentrations of SPIONs (5, 10, 25, 50, and 100 µg/mL) for 24 and 48 h; 4- Cells treated with both methods (different concentrations of SPION + ELMF).

In all the groups, after the treatment was completed, the culture medium was removed and replaced with 100 µL of 0.5 mg/mL MTT or tetrazolium salt (serum-free), and then, the plates were incubated in 5% CO₂ at 37 °C for 4 h. Reduction of the yellow tetrazolium salt (MTT) by mitochondrial and cytosolic dehydrogenases of living cells consequently led to the production of insoluble precipitate purple formazan dye. Since the precipitated purple formazan was insoluble, the supernatant was removed and the remaining blue precipitate of each well was solubilized in 100 µL of DMSO. The color intensity of the plates was measured at 540 nm using the BioTek ELx808 microplate reader. The amount of purple color produced in this test was directly proportional to the number of viable and metabolically active cells.

Statistical Analysis

The results were expressed as the mean ±standard deviation (SD). The significance of the differences between the treated groups was evaluated by the one-way ANOVA using the GraphPad Prism 6 software. A P value <0.05 was considered statistically significant using the confidence interval of 95%.

RESULTS

The Synthesis and Characterization of Nanoparticles The synthesized nanoparticles were characterized by using different techniques. DLS results showed that the particle size distribution was about 32 nm, and the surface charge of the synthesized particles was -19 mV (Figure 2a, b). The XRD pattern showed that SPIONs had a pure crystalline structure without any impurity (Figure 3). The magnetic feature of the

SPIONs was confirmed by vibrating sample magnetometry (VSM). Magnetization (emu/g) as a function of applied field (Oe) at room temperature is depicted in Figure 4. The magnetization curve demonstrated that the nanoparticles possessed the magnetic saturation (MS) of about 66.9 emu/g. These findings showed that the synthesized nanoparticles exhibited superparamagnetic behavior and the magnetic particle saturation was very good against the external magnetic field intensity.

Cell Viability

MTT assay results revealed that the percentage of viable cells in the group exposed to ELMF for 24 and 48 h was decreased, compared with the control group, and reached 89.22% \pm 4.40% and 85.82% \pm 3.89%, respectively. Also, the results showed that SPIONs at lower concentrations (5, 10 and 25 μ g/mL) were not capable of inducing cytotoxicity at 24 h ($P \geq 0.05$). However, high concentrations of SPIONs (50 and 100 μ g/mL) decreased cell viability and induced cell death ($P \leq 0.05$). This increment was enhanced at 48 h; therefore, the viability of cells significantly decreased at 10 and 25 μ g/mL concentrations of SPIONs. The high concentrations of SPIONs at both 24 and 48 h induced cell death and reduced cell viability (Figure 6a, b). In the group treated with both ELMF and SPIONs, the cell viability was significantly reduced compared with the SPION-only (at all concentrations of SPIONs) and control groups. These results showed that ELMF in the presence of SPION synergistically induced cell death.

The percentage of the cell viability of the groups that were treated only with different concentrations of SPION (5, 10, 25, 50, and 100 μ g/mL) and SPION-

N+ELMF were 14.24%, 16.43%, 32.08%, 22.04% and 26.39% in 24 h and 15.92%, 13.76%, 22.42%, 23.44% and 35.50% in 48 h, respectively. These results showed a significant difference in the mortality between each treatment alone and that of SPION+ELMF, which had a synergistic effect on the induced cell death by SPIONs. Therefore, ELMF at low frequency (50 Hz) and high exposure time could be used as a new procedure to induce the death of cancer cells and this method could be used as an alternative to hyperthermia.

DISCUSSION

In an attempt to enhance the quality of hyperthermia as a treatment option and to avoid overheating, a new alternative approach was introduced in which the frequency was decreased while the exposure time was prolonged. As shown in Figure 6, high concentrations of SPIONs were toxic for cells and increased cell death and reduced their viability. In addition, ELMF alone, at 24 and 48 h, induced cell death and decreased cell viability, compared with the control group. The cell mortality rates were increased significantly in the ELMF+SPION group compared with those groups that were given individual treatments. SPIONs because of their very small size were more likely to be absorbed in cells compared with larger magnetic nanoparticles. We can, therefore, consider that their increased absorption leads to their enhanced action [23]. On the other hand, the DLS results showed that the surface charge of SPIONs was negative, which could be due to adsorption of hydroxyl ions (OH^-) onto the surface in the aqueous medium.

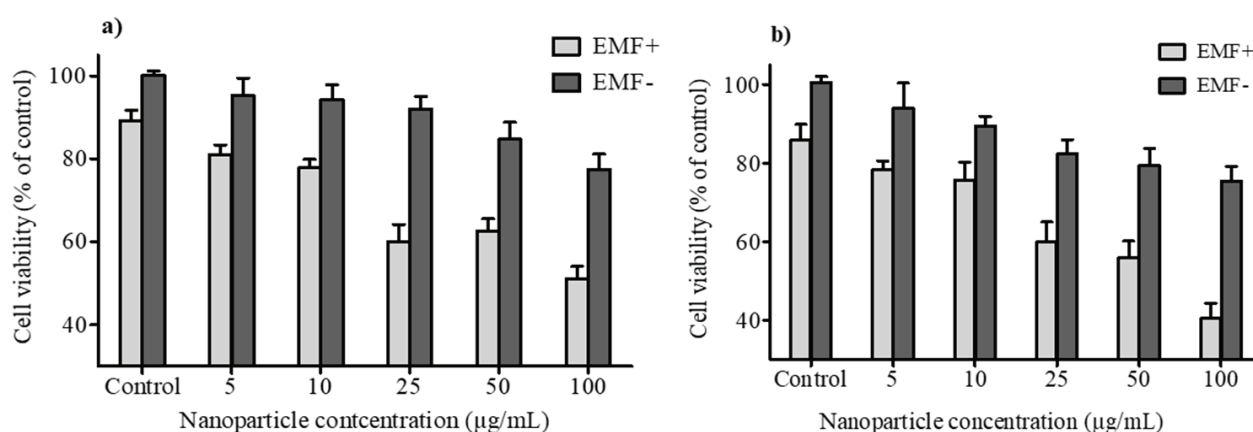


Figure 6: Effect of Various Concentrations of SPIONs on the Viability of MCF-7 Cells in the Presence and Absence of EMF at a Frequency of 50 Hz and an Intensity of 20 mT Exposed for a) 24 h and b) 48 h

This negative charge causes the adsorption of positively charged ions and proteins, and consequently reduced the activity of the functional proteins in the living system [24]. Another report also showed that SPIONs can increase the concentration of free radicals in the cells, thereby inducing apoptosis [25]. Magnetic nanoparticles at high concentrations affected cellular skeleton proteins, including actin and other adherent proteins thereby reducing cell proliferation [26].

The findings from the present study indicated that ELMF increased cell death. These results are supported by previous reports pertaining to the biological effects of ELMF [27]. For example, it was reported that EMF can increase the concentration of free radicals through the Fenton reaction, which damaged biomolecules such as the DNA and induced cell death [28, 29]. In fenton reaction hydroxyl radical is produced from hydrogen peroxide in the presence of ferrous iron:



Another study showed that EMF at a 2-mT intensity and 50 Hz frequency increased intracellular cAMP and inhibited cell proliferation [30]. Another report showed that a 50-Hz EMF reduced the antioxidant defense system significantly in the mouse brain [31]. Generally, EMF through thermal and non-thermal effects can influence living organisms in different ways such as: cell and organ rotation, cell membrane degradation, the permeability of the membrane, membrane transition, biochemical reactions and behavior of charged ions and molecules through the applied force [32, 33]. The molecular changes induced by EMF lead to larger biological manifestations such as cell death, necrosis, and apoptosis [34]. In addition, EMF, by affecting calcium ion flow in cell membranes and organelles, led to apoptosis induction, thereby causing increased cell death [35]. These bioeffects happened through various mechanisms.

The present study reported that EMF+SPIONs synergistically decreased cell viability and increased cell death. The magnetic nanoparticles subjected to a variable magnetic field generate heat due to the Brownian and Neel relaxation [36]. The amount of heat depends on the characteristics of the applied field and the nature and size of the nanoparticles [37]. Many *in vitro* and *in vivo* studies, which examined the process, have confirmed the hypothesis [30–32]. The studies have shown that heat and EMF have a strong synergis-

tic impact on the death of tumor cells [34]. Therefore, the increased cell death in the EMF+SPIONs method can be explained as follows: each of these treatments had a nonthermal effect on the living system, but the effect of the combined treatment was enhanced. Moreover, thermal effects and heat generation that occurred in the combined treatment was responsible for the observed biological effects. Indeed, the generated heat and EMF synergistically increased cell death. MTT assay was used to determine the viability of cells but the type of cell death was not determined. The authors intend to prove the findings by using apoptosis kits or LDH assay in future studies.

ACKNOWLEDGMENTS

This work was supported by a grant no 93010102 from Iran National Science Foundation (INSF).

CONFLICTS OF INTEREST

The authors claimed that there is no conflict of interest regarding this paper.

ETHICS APPROVAL

Not applicable.

REFERENCES

1. Zaitsev VS, Filimonov DS, Presnyakov IA, Gambino RJ, Chu B. Physical and Chemical Properties of Magnetite and Magnetite-Polymer Nanoparticles and Their Colloidal Dispersions. *J Colloid Interface Sci.* 1999;212(1):49-57. <https://doi.org/10.1006/jcis.1998.5993>.
2. Schlorf T, Meincke M, Kossel E, Glüer CC, Jansen O, Mentlein R. Biological properties of iron oxide nanoparticles for cellular and molecular magnetic resonance imaging. *Int J Mol Sci.* 2010;12(1):12–23. <https://doi.org/10.3390/ijms12010012> PMID:21339973
3. Li L, Jiang W, Luo K, Song H, Lan F, Wu Y et al. Superparamagnetic iron oxide nanoparticles as MRI contrast agents for non-invasive stem cell labeling and tracking. *Theranostics.* 2013;3(8):595–615. <https://doi.org/10.7150/thno.5366> PMID:23946825
4. Chen B, Wu W, Wang X. Magnetic iron oxide nanoparticles for tumor-targeted therapy. *Curr Cancer Drug Targets.* 2011;11(2):184–9. <https://doi.org/10.2174/156800911794328475> PMID:21158723
5. Hamaguchi T, Kato K, Yasui H, Morizane C, Ikeda M, Ueno H, et al. A phase I and pharmacokinetic study of NK105, a paclitaxel-incorporating micellar nanoparticle formulation. *Br J Cancer.* 2007;97(2):170-6. <https://doi.org/10.1038/sj.bjc.6603855> PMC2360299.
6. Shi Y, Zhou L, Wang R, Pang Y, Xiao W, Li H, et al. In situ preparation of magnetic nonviral gene vectors and magnetofection *in vitro*. *Nanotechnology.* 2010;21(11):

115103. <https://doi.org/10.1088/0957-4484/21/11/115103>.
7. Kami D, Takeda S, Itakura Y, Gojo S, Watanabe M, Toyoda M. Application of magnetic nanoparticles to gene delivery. *Int J Mol Sci*. 2011;12(6):3705–22. <https://doi.org/10.3390/ijms12063705> PMID:21747701
 8. Siegel RL, Miller KD, Jemal A. Cancer statistics, 2016. *CA Cancer J Clin*. 2016;66(1):7–30. <https://doi.org/10.3322/caac.21332> PMID:26742998
 9. Zeichner SB, Terawaki H, Gogineni K. A review of systemic treatment in metastatic triple-negative breast cancer. *Breast Cancer (Auckl)*. 2016;10:25–36. <https://doi.org/10.4137/BCBCR.S32783> PMID:27042088
 10. Wang Y, Zhang T, Kwiatkowski N, Abraham BJ, Lee TI, Xie S et al. CDK7-dependent transcriptional addiction in triple-negative breast cancer. *Cell*. 2015; 163(1): 174–86. <https://doi.org/10.1016/j.cell.2015.08.063> PMID:26406377
 11. Musgrove EA, Sutherland RL. Biological determinants of endocrine resistance in breast cancer. *Nat Rev Cancer*. 2009;9(9):631–43. <https://doi.org/10.1038/nrc2713> PMID:19701242
 12. Cleator SJ, Ahamed E, Coombes RC, Palmieri C. A 2009 update on the treatment of patients with hormone receptor-positive breast cancer. *Clin Breast Cancer*. 2009;9 Suppl 1:S6–17. <https://doi.org/10.3816/CBC.2009.s.001> PMID:19561006
 13. Phillips JL, Singh NP, Lai H. Electromagnetic fields and DNA damage. *Pathophysiology*. 2009;16(2-3):79–88. <https://doi.org/10.1016/j.pathophys.2008.11.005> PMID:19264461
 14. Pall ML. Electromagnetic fields act via activation of voltage-gated calcium channels to produce beneficial or adverse effects. *J Cell Mol Med*. 2013;17(8):958–65. <https://doi.org/10.1111/jcmm.12088> PMID:23802593
 15. Barbault A, Costa FP, Bottger B, Munden RF, Bomholt F, Kuster N, et al. Amplitude-modulated electromagnetic fields for the treatment of cancer: discovery of tumor-specific frequencies and assessment of a novel therapeutic approach. *J Exp Clin Cancer Res*. 2009;28:51. <https://doi.org/10.1186/1756-9966-28-51> PMC2672058.
 16. Williams CD, Markov MS, Hardman WE, Cameron IL. Therapeutic electromagnetic field effects on angiogenesis and tumor growth. *Anticancer Res*. 2001;21(6A):3887-91. PMID: 11911264
 17. Jadhav NV, Prasad AI, Kumar A, Mishra R, Dhara S, Babu KR, et al. Synthesis of oleic acid functionalized Fe₃O₄ magnetic nanoparticles and studying their interaction with tumor cells for potential hyperthermia applications. *Colloids Surf B Biointerfaces*. 2013;108:158-68. <https://doi.org/10.1016/j.colsurfb.2013.02.035> PMID: 23537834
 18. Pollert E, Veverka P, Veverka M, Kaman O. Search of new core materials for magnetic fluid hyperthermia: preliminary chemical and physical issues. *Prog. Solid State*; 2009.
 19. Granov AM, Muratov OV, Frolov VF. Problems in the Local Hyperthermia of Inductively Heated Embolized Tissues. *Theor Found Chem Eng*. 2002;36(1):63–6. <https://doi.org/10.1023/A:1013901625389>
 20. Huber DL. Synthesis, properties, and applications of iron nanoparticles. *Small*. 2005;1(5):482–501. <https://doi.org/10.1002/sml.200500006> PMID:17193474
 21. Krishnan KM. Biomedical nanomagnetism: a spin through possibilities in imaging, diagnostics, and therapy. *IEEE Trans Magn*. 2010;46(7):2523–58. <https://doi.org/10.1109/TMAG.2010.2046907> PMID:20930943
 22. Lu AH, Salabas EL, Schüth F. Magnetic nanoparticles: synthesis, protection, functionalization, and application. *Angew Chem Int Ed Engl*. 2007;46(8):1222–44. <https://doi.org/10.1002/anie.200602866> PMID:17278160
 23. Huang J, Bu L, Xie J, Chen K, Cheng Z, Li X et al. Effects of nanoparticle size on cellular uptake and liver MRI with PVP-coated iron oxide nanoparticles. *ACS Nano*. 2010. <https://doi.org/10.1021/nn101643u>.
 24. Ge Y, Zhang Y, Xia J, Ma M, He S, Nie F et al. Effect of surface charge and agglomerate degree of magnetic iron oxide nanoparticles on KB cellular uptake in vitro. *Colloids Surf B Biointerfaces*. 2009 Oct;73(2):294–301. <https://doi.org/10.1016/j.colsurfb.2009.05.031> PMID:19564099
 25. Naqvi S, Samim M, Abdin M, Ahmed FJ, Maitra A, Prashant C et al. Concentration-dependent toxicity of iron oxide nanoparticles mediated by increased oxidative stress. *Int J Nanomedicine*. 2010 Nov;5:983–9. <https://doi.org/10.2147/IJN.S13244> PMID:21187917
 26. Soenen SJ, Nuytten N, De Meyer SF, De Smedt SC, De Cuyper M. High intracellular iron oxide nanoparticle concentrations affect cellular cytoskeleton and focal adhesion kinase-mediated signaling. *Small*. 2010 Apr;6(7): 832– 42. <https://doi.org/10.1002/sml.200902084> PMID:20213651
 27. Haghghat N, Abdolmaleki P, Behmanesh M, Satari M. Stable morphological-physiological and neural protein expression changes in rat bone marrow mesenchymal stem cells treated with electromagnetic field and nitric oxide. *Bioelectromagnetics*. 2017;38(8):592-601. <https://doi.org/10.1002/bem.22072>.
 28. Blank M, Goodman R. DNA is a fractal antenna in electromagnetic fields. *Int J Radiat Biol*. 2011;87(4):409–15. <https://doi.org/10.3109/09553002.2011.538130> PMID:21457072
 29. Phillips JL, Haggren W, Thomas WJ, Ishida-Jones T, Adey WR. Magnetic field-induced changes in specific gene transcription. *Biochim Biophys Acta*. 1992;1132(2):140-4. [https://doi.org/10.1016/0167-4781\(92\)90004-J](https://doi.org/10.1016/0167-4781(92)90004-J).
 30. Koziorowska A, SOLEK P, MAJCHROWICZ L, ROMEROWICZ-MISIELAK M. The impact of electromagnetic fields with frequency of 50 Hz on metabolic activity of cells in vitro. *Przegląd Elektrotechniczny*. 2017; 5;93(1):161-4.
 31. Falone S, Mirabilio A, Carbone MC, Zimmitti V, Di Loreto S, Marigliò MA et al. Chronic exposure to 50Hz magnetic fields causes a significant weakening of antioxidant defence systems in aged rat brain. *Int J Biochem Cell Biol*. 2008;40(12):2762–70. <https://doi.org/10.1016/j.biocel.2008.05.022> PMID:18585472
 32. Kaiser DF. Theoretical physics and biology: non-linear dynamics and signal amplification—relevant for EMF in-

- teraction with biological systems?. In Proceedings of the Workshop on Proposed Mechanisms for the Interaction of RF-Signals with Living Matter: Demodulation in Biological Systems 2006 Sep.
33. Hardell L, Sage C. Biological effects from electromagnetic field exposure and public exposure standards. *Biomed Pharmacother.* 2008;62(2):104–9. <https://doi.org/10.1016/j.biopha.2007.12.004> PMID:18242044
 34. Repacholi MH, Greenebaum B. Interaction of static and extremely low frequency electric and magnetic fields with living systems: health effects and research needs. *Bioelectromagnetics.* 1999; 20 (3): 133–60. [https://doi.org/10.1002/\(SICI\)1521-186X\(1999\)20:3<133::AID-BE-M1>3.0.CO;2-O](https://doi.org/10.1002/(SICI)1521-186X(1999)20:3<133::AID-BE-M1>3.0.CO;2-O) PMID:10194557
 35. Pall ML. Electromagnetic fields act via activation of voltage-gated calcium channels to produce beneficial or adverse effects. *J Cell Mol Med.* 2013;17(8):958–65. <https://doi.org/10.1111/jcmm.12088> PMID:23802593
 36. Jordan A, Wust P, Fahling H, John W, Hinz A, Felix R. Inductive heating of ferrimagnetic particles and magnetic fluids: physical evaluation of their potential for hyperthermia. *Int J Hyperthermia.* 1993;9(1):51-68. PMID: 8433026
 37. Li W, Liu Y, Qian Z, Yang Y. Evaluation of Tumor Treatment of Magnetic Nanoparticles Driven by Extremely Low Frequency Magnetic Field. *Sci Rep.* 2017;7:46287. <https://doi.org/10.1038/srep46287>. PMC5387737.